# Flux balance analysis of genome-scale metabolic model of rice (*Oryza sativa*): Aiming to increase biomass

RAHUL SHAW and SUDIP KUNDU*

*Department of Biophysics, Molecular Biology and Bioinformatics, University of Calcutta, 92 APC Road,
Kolkata 700009, India*

*Corresponding author (Email, skbmbg@caluniv.ac.in)*

Due to socio-economic reasons, it is essential to design efficient stress-tolerant, more nutritious, high yielding rice varieties. A systematic understanding of the rice cellular metabolism is essential for this purpose. Here, we analyse a genome-scale metabolic model of rice leaf using Flux Balance Analysis to investigate whether it has potential metabolic flexibility to increase the biosynthesis of any of the biomass components. We initially simulate the metabolic responses under an objective to maximize the biomass components. Using the estimated maximum value of biomass synthesis as a constraint, we further simulate the metabolic responses optimizing the cellular economy. Depending on the physiological conditions of a cell, the transport capacities of intracellular transporters (ICTs) can vary. To mimic this physiological state, we randomly vary the ICTs' transport capacities and investigate their effects. The results show that the rice leaf has the potential to increase glycine and starch in a wide range depending on the ICTs' transport capacities. The predicted biosynthesis pathways vary slightly at the two different optimization conditions. With the constraint of biomass composition, the cell also has the metabolic plasticity to fix a wide range of carbon-nitrogen ratio.

## 1. Introduction

Rice, a staple food, is referred to as 'life' for half of the world's human population (Fresco 2005). While more than 30% of the total caloric intake of the Asians comes from rice, nearly three billion people of the world intake rice as their major food (Gnanamanickam 2009). Thus, food security for billions of people, especially in the developing countries, is a critical issue. On the other hand, this important crop is under several biotic and abiotic stresses which decrease the production of rice and thus increase the risk of starvation in several parts of the world (Parry *et al.* 2004). The challenge remains in designing a high-yielding more nutritious rice cultivar. Researchers are trying to meet this need through different approaches. For example, several important genes were identified from the wild varieties to improve the yield and quality of modern rice (Jinhua *et al.* 1996). Ideotype approach and crossing between different varieties have been used to increase the biomass of hybrid rice (Peng *et al.* 2008). Another notable advancement is made in

producing vitamin A–enriched golden rice (Beyer *et al.* 2002). On the other hand, metabolic engineering has been proven as a powerful technique for over or less production of specific metabolites in microbes (Peralta-Yahya *et al.* 2012). Modelling and analysis of the cellular metabolism is a key step in the success of metabolic engineering. So, the plant biologists are also trying to understand the plant's systems level biochemistry at normal as well as perturbed conditions (Poolman *et al.* 2009, 2013; Simons *et al.* 2014).

A cell can be considered as a biochemical machinery that produces necessary biomass and energy needed for the survival, maintenance and growth of a species. The response of this biochemical machinery under varying conditions to which the cell is exposed can be studied through metabolic modelling. There are two broad classes of metabolic modelling techniques: one is structural and the other is kinetic. Due to lack of enzyme kinetics data (Schuster and Fell 2007), kinetic modelling is normally used for small metabolic pathways. On the other hand, structural modelling depends on the balanced (in atom and mass) reaction stoichiometry and thermodynamically feasible directionality of the reactions. A large number of available genomes helped researchers to build genome-scale metabolic models. Flux balance analysis (FBA) is widely used to study these genome-scale metabolic networks (Edwards *et al.* 2002; Varma and Palsson, 1994; Herrgard *et al.* 2008; Poolman *et al.* 2009, 2013; Simons *et al.* 2014). In FBA, the method aims to optimize an objective function under the given constraints. The solution space can vary depending on the constraints as well as the optimization criteria (Cheung *et al.* 2013). On the other hand, it has been already demonstrated that depending on the cellular needs and environmental conditions, every species can use different metabolic strategies for its survival and growth (*Sweetlove et al.* 2010; Shaw and Kundu 2013).

A partially compartmentalized genome-scale metabolic model of rice leaf has already been reported and the metabolic response of this model at varying light intensities has also been observed (Poolman *et al*. 2013). Several realistic physiological states of rice leaf are reported there. The minimization of the total cellular flux (i.e. optimization of the cellular economy) has been used as objective function. The metabolic responses are simulated at steady state condition and the constraints used in that analysis include a fixed ratio of different biomass precursors (amino acids, nucleotides, lipid, starch, sucrose, cellulose and lignin).

Recently, we have simulated the responses of rice leaf metabolism to observe the effect of intracellular transporters' transport capacities (Shaw and Kundu 2013). The analysis predicts different modes of tricarboxylic acid (TCA) cycle that can be used by the rice plant due to variation in transport capacities. It also suggests the minimum amount of photon needed to synthesize the biomass in experimentally observed proportion varies in a wide range.

Here, our major focuses are (i) whether the rice leaf has the metabolic potential to maximize any of the biomass precursors, (ii) if so, prediction of the possible pathway using two different objective functions namely (a) maximization of biomass and (b) maximization of the cellular economy, and (iii) comparison of these pathways. As the carbon (C) and nitrogen (N) fixation pathways of a cell are interlinked, it is expected that there might be a lower and upper limit of C/N ratio in biomass composition. Here, we have predicted the variation of C/N ratio. Some of the metabolites produced in one sub-cellular compartment can be transported to other compartments. The transport of these depends on the existence of intracellular transporters and on their transport capacities. While simulating the metabolic responses, we vary the transporters' transport capacities to understand their effects as well.

## 2. Materials and methods

### 2.1 *Metabolic model*

We have used the partially compartmentalized (having compartments: chloroplast, mitochondria and cytosol) genome-scale metabolic model of rice (*Oryza sativa*) leaf (Poolman *et al.* 2013). This model contained 1736 reactions and 1484 metabolites. In principle, all the substrates and products of any reaction (other than reactions representing biomass precursors and nutrients) should be produced and consumed, respectively by another reaction in a metabolic model. If either the substrates or the products of a reaction was not produced or consumed by any other reaction, then the reaction was termed as 'dead reaction' (Poolman *et al.* 2006). We find that there are 710 dead reactions. We curated the previously published model by removing these dead reactions.

The curated model used in this work contains 1026 reactions and 686 metabolites. Among 1026 reactions, 22 were intracellular transporters (ICTs) that were used to exchange fluxes within intracellular organelles present in the model. The stoichiometry matrix

$$\mathbf{S}(m \times n) \tag{1}$$

was constructed, where $m$ is the number of metabolites and $n$ is number of reactions. In steady state

$$\mathbf{S}.\mathbf{v} = 0 \tag{2}$$

where $\mathbf{v}$ is the flux vector of reactions (Kauffman *et al.* 2003). Objective function is

$$\mathbf{Z} = \mathbf{w}.\mathbf{v} \tag{3}$$

where **w** is the weight vector of the reactions. Objective function (**Z**) can be maximized ($Z_{Max}$) or minimized ($Z_{Min}$):

$$\text{Subject to} = \begin{cases} \mathbf{S.v} = 0 \\ \alpha_i \le \mathbf{v}_i \le \beta_i \end{cases} \quad (4)$$

Here, $\alpha_i$ and $\beta_i$ are the lower and upper bounds on reaction flux $\mathbf{v}_i$, respectively. The flux balance analysis (Edwards *et al.* 2002; Orth *et al.* 2010) optimizes the objective function using mainly linear programming (LP) to find steady state fluxes under given constraints. The nutrients we have used are carbon dioxide, oxygen, nitrate, ammonia, sulphate, phosphate and water. We also added a transporter that transports external photon to the cell for modelling purpose. This photon was utilized in cyclic and non-cyclic photophosphorylation within the chloroplast of the cell. We have considered all the amino acids, nucleotides, lipid, starch, sucrose, cellulose and lignin as biomass precursors.

## 2.2 *Optimization criteria*

We have used two types of optimization criteria. To identify the possibility of overproduction of biomass, we optimized all the biomass components. The lower value of each biomass component was fixed to the experimentally observed proportion present in the rice leaf (Poolman *et al.* 2013). Here, the effort was to identify the possibility of overproduction of any biomass component while constraining the minimum production of other biomass components. We refer this optimization criterion as biomass optimization ($Z_{Max}$).

In another set of analysis, we fixed the highest value of biomass component, if any, observed in a previous analysis and then optimizes the cellular economy, i.e. the minimization of the sum of fluxes of all reactions under study. We refer this optimization criterion as optimization of cellular economy ($Z_{Min}$).

## 2.3 *Introducing the effect of intracellular transporters*

The weight of each intracellular transporter was varied randomly from 0 to 1000. We simulated the metabolic responses for 1000 iterations. In each iteration, the weights of ICTs would capture the transporters' transport capacities. It is recommended that if the upper and lower limits of the flux of any reaction are unknown, then one can use arbitrary large values of flux and simulate the responses using FBA (Vo *et al.* 2004). There is no experimental value providing allowable range of the flux through ICTs. However, it is known that the transport capacity can vary depending on the environmental conditions. To mimic this physiological situation, we considered the following conditions: (i) the flux of

ICTs can take any arbitrary flux value up to 100 and (ii) the weights of ICTs can vary as mentioned earlier. Moreover, these are further constrained by the nutrients uptake, biomass composition and optimization criteria. Depending on the weights imposed on ICTs, each iteration would generate a possible solution. These possible solutions (metabolic pathways) would represent different intracellular metabolite transport environments within a cell.

## 2.4 *Other constraints*

Nutrients uptake and photon flux were free to use any value ($\ge 0$). A cell maintenance cost was assumed to 0.1 flux unit through a generic ATPase reaction (Poolman *et al.* 2013).

## 2.5 *Implementation and analysis*

The method was implemented and analysed using ScrumPy metabolic modelling tool (Poolman 2006) with modules written in Python programming language. The algorithms for maximization ($Z_{Max}$) and minimization ($Z_{Min}$) of the objective are described as Algorithm 1 and 2, respectively.

**Algorithm 1**: Algorithm to observe maximization of the biomass production when ICT's transport capacity changes. The algorithm here is shown only for a single iteration. Running 1000 iterations of this algorithm provides the solution space of our use. The results are bound to the constraints we used here.

1. **Start**
2. Load Model *//From a ScrumPy model file*
3. Build Linear Programming (LP) Object *//Include model in glpk*
4. Set Constraints of LP *//Lower (l) and upper (u) bound of fluxes*

$$C_{LP} = \begin{cases} l \leftarrow 0, u \leftarrow + \text{AV for irreversible reaction} \\ l \leftarrow -\text{AV}, u \leftarrow + \text{AV for reversible reaction} \end{cases}$$

*//AV is Any Value of fluxes*

5. Set $l \leftarrow$ Experimentally observed proportion and $u \leftarrow$ AV for biomass precursors
6. Set $l \leftarrow 0$ and $u \leftarrow 100$ (an arbitrary maximum value) for ICTs *//Flux bound to ICTs, part of $C_{LP}$*
7. Set Objective to Maximize Biomass ($Z_{Max}$) *//Maximize biomass precursor fluxes*
8. T = List of Intracellular Transporters *//Includes 22 intracellular transporters*

**for** i = 1 to cardinality of T **do**
$w_{Ti} \leftarrow$ A random integer in [0,1000] *//used uniform integer distribution*
**end for** *//Random weight assignment on all ICTs is complete*

9. Solve LP Using Simplex Method *//To get flux distributions*

10. Get Solution *//Reactions with their respective fluxes*

11. **End**

**Algorithm 2**: Algorithm to observe the cellular economy.

**1. Start**

2 - 4. = Steps similar to steps 2 - 4 in Algorithm 1

5. Fix Biomass Fluxes *//Obtained from biomass optimization process*

6. Set Objective to Minimize all Reactions Fluxes ($Z_{Min}$) *//Optimize cellular economy*

7. = Step 9 in Algorithm 1

8. = Step 10 in Algorithm 1

9. **End**

### 3. Results

#### 3.1 *General responses*

We have observed that nearly half of the reactions (486) of the whole metabolic model were present in the solution space under biomass optimization criteria and these reactions have been used to maximize the biomass. A total of 182 reactions always remain active when we vary the transporter's transport capacity. This suggests that the rice leaf metabolism uses these 182 reactions as a core set to optimize its biomass; on the other hand, the plant would find alternative paths if any of the remaining 304 reactions is deleted.

#### 3.2 *Overproduction of biomass components*

We simulated the metabolic responses for optimization of biomass components. The fluxes of the biomass transporters were included in the objective function and their lower values were fixed to experimentally observed proportions.

We observed that the system prefers to overproduce only starch and glycine among all biomass components as shown in figure 1. We also observed that starch and glycine overproduction would vary depending on the weights imposed on intracellular transporters. It is worthy to mention that intracellular transporter's transport capacity could vary depending on cellular condition (Shaw and Kundu 2013). Thus, it is evident from figure 1 that if the plant is trying to optimize its biomass production depending on the transporter's activity, the plant has different capacities to overproduce its biomass components.

*3.2.1 Preferred metabolic path of starch metabolism under biomass optimization:* We have implemented Algorithm 1,



**Figure 1.** Flux distributions for starch and glycine transporters in the entire range of observations. X (Flux) and Y (Frequency) axes represent the flux (in mole) and number of occurrence of a particular flux value in the entire simulation, respectively. Maximum flux through starch transporter was 16.65 flux unit and occurred 154 number of times, whereas that for glycine was 47.59 and occurred only once. Minimum values of fluxes were 0.00011 and $2.1 \times 10^{-05}$ for starch and glycine, respectively.

where we set the lower values of biomass precursors at experimentally observed values [values are taken from (Poolman *et al.* 2013)] and randomized the weight of intracellular transporters. Using the biomass optimization criteria, we predict the maximum value of starch that can be synthesized for this metabolic model. Then, to remove the imposed constraint on ICTs, we set equal weight (**w** = 1) for each of the intracellular transporters. We simulated the responses for two different values of biomass precursors (i) fixing the flux of starch to the maximum value as observed in previous solution and (ii) fixing the minimum value of starch. In both the cases, the biomass components other than starch are fixed to their experimentally observed proportions. Then we simulate the metabolic responses under biomass optimization criteria and identified the possible preferred pathways. These maximum and minimum starch biosynthesis pathways and the flux distributions are shown in figure 2. We observe some differences between these two metabolic paths. For example, chloroplastidal F6P to G6P conversion is only active when the plant produces minimum starch. Chloroplastidial G6P transporter transports carbon compound from chloroplast to cytosol in minimum starch production pathway; but during overproduction of starch, this transporter transports G6P from cytosol to chloroplast. A major fraction of $C_3$
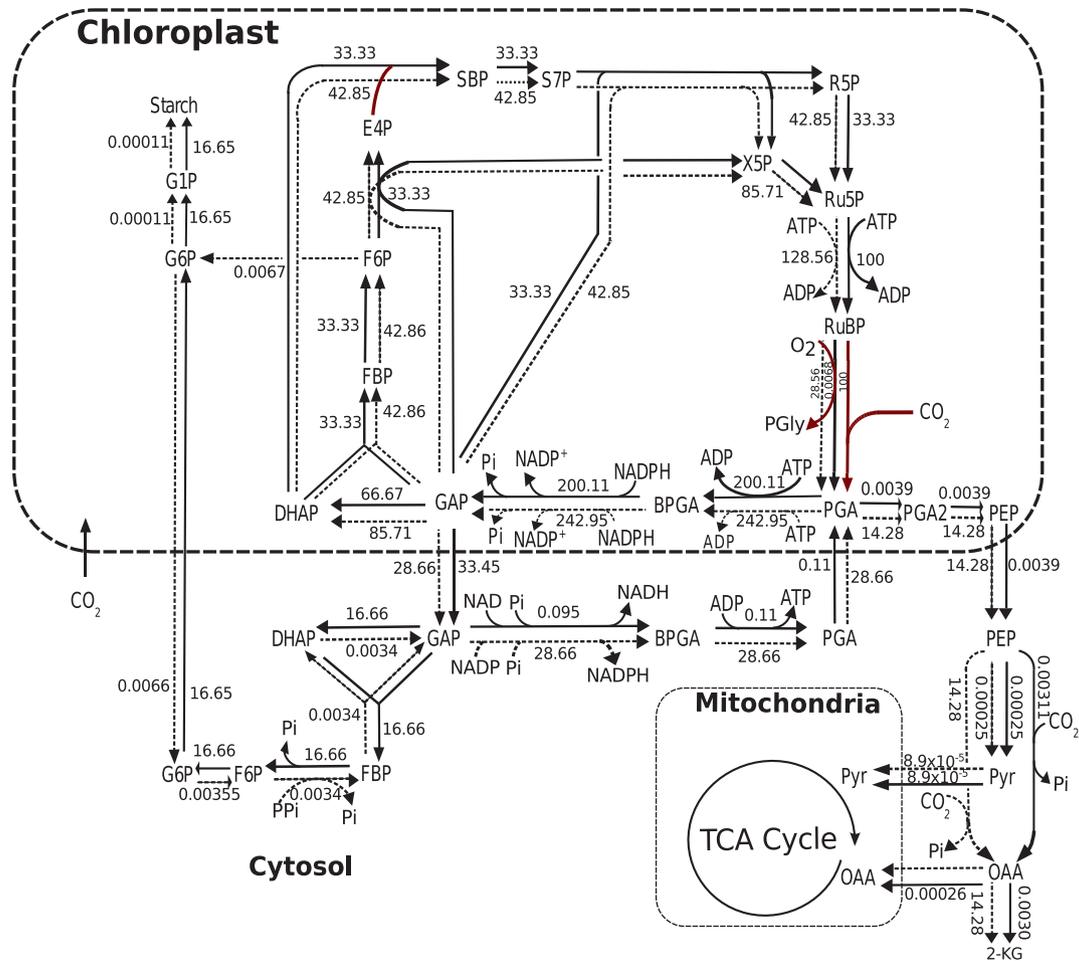
**Figure 2.** Flux distributions for high (solid) and low (dashed) starch production in the central carbon metabolism. Numbers on the reactions are the flux values (we use this type of flux value representation in all other figures hereafter). All the reactions are not included. Brown lines are common to both flux modes.

intermediates is transported from chloroplast to cytosol via GAP transporter in both the cases. In case of starch overproduction, a major fraction of the cytosolic GAP is converted to G6P that is transported again to chloroplast to overproduce starch. On the other hand, in case of minimum starch production, the cytosolic GAP is mostly converted to cytosolic PGA that again is transported to chloroplast and makes a cycle.

3.2.2 *Starch metabolism in cellular economy optimization:* Next, we fixed the highest value of starch (observed in biomass optimization criteria) in the model and other biomass components are fixed in the experimentally observed values. Then, the cellular economy ($Z_{Min}$) was optimized. Under this optimization criterion, the

predicted path is shown in figure 3. Interestingly, this path is almost similar (with few exceptions) to the path shown in figure 2 (dashed line). The exception lies in the difference of G6P transporter's activity. In addition, to achieve the cellular economical condition, most of the chloroplastidial GAP is utilized within the chloroplast via F6P production to produce the maximum amount of starch. Another notable difference lies in the pathway of cytosolic pyruvate production which is further utilized in the truncated TCA cycle of mitochondria. The source of cytosolic pyruvate in biomass optimized condition is the chloroplastidial PEP which is transported into the cytosol and converts into pyruvate. On the other hand, when the cell is trying to optimize its economy, cytosolic GAP is converted into PEP via PGA and 2-PG
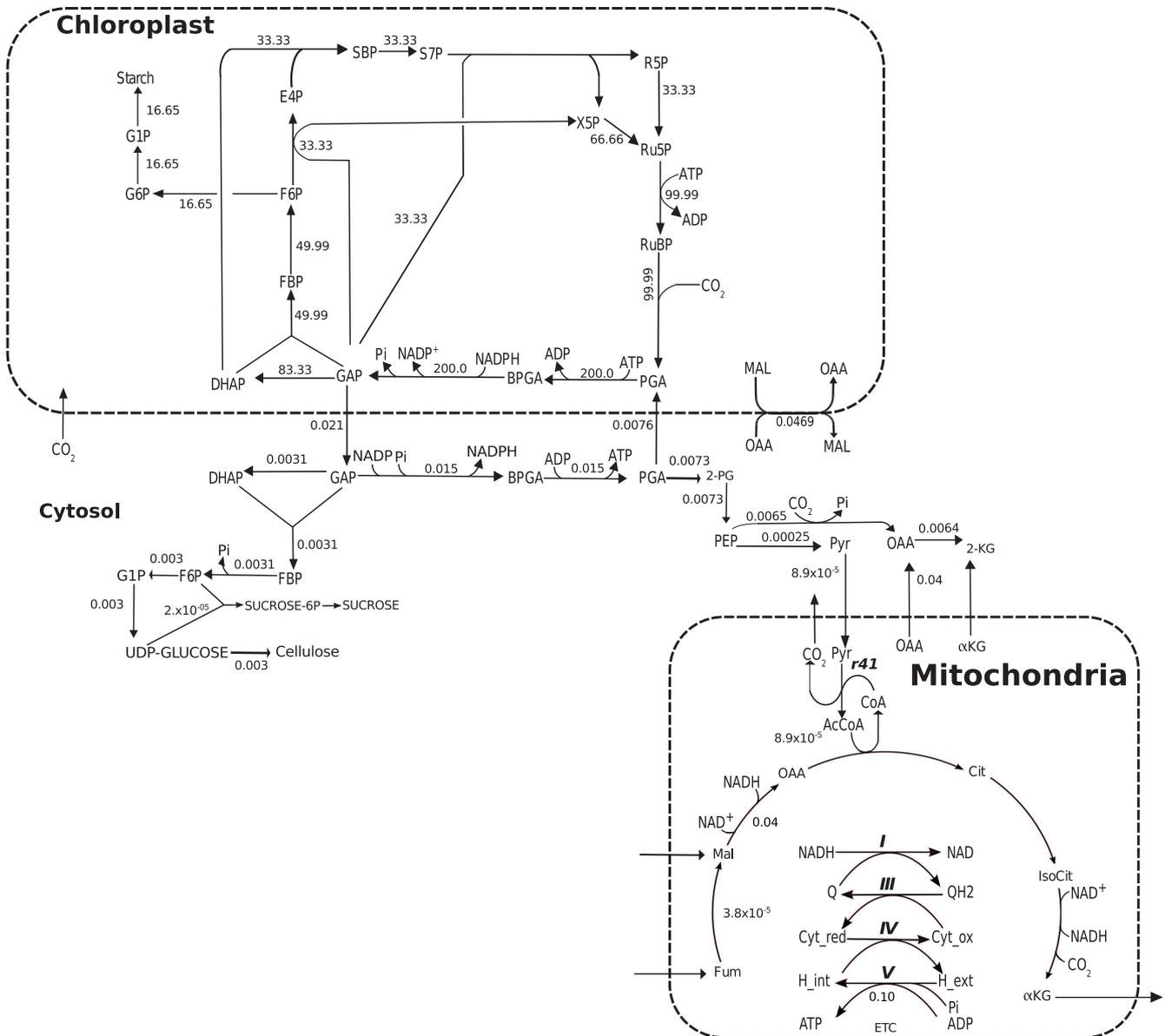
**Figure 3.** Starch synthesis pathway when the flux of starch is set to its maximum value and the objective is set to optimize cellular economy. ETC in the mitochondria represents the electron transport chain.

production. The participation of non-cyclic TCA cycle is also shown in figure 3. We should mention that it was demonstrated that the TCA cycle can operate in different truncated modes depending on the cellular need and condition (Sweetlove *et al*. 2010).

3.2.3 *Glycine metabolism in biomass optimization:* The glycine (Gly) biosynthesis pathways observed under biomass optimization criteria are shown in figure 4. It represents maximum and minimum glycine production pathways. The chloroplastidial $C_3$ intermediates, which are ultimately utilized in Gly biosynthesis in cytosol, are transported via PEP (in both maximum and minimum Gly synthesis) and PGA (minimum Gly biosynthesis). Next, we discuss the pathway followed in maximum Gly biosynthesis under biomass optimization criteria. The cytosolic phosphoenol pyruvate carboxylase converts PEP to OAA. Then the degradation of GLT
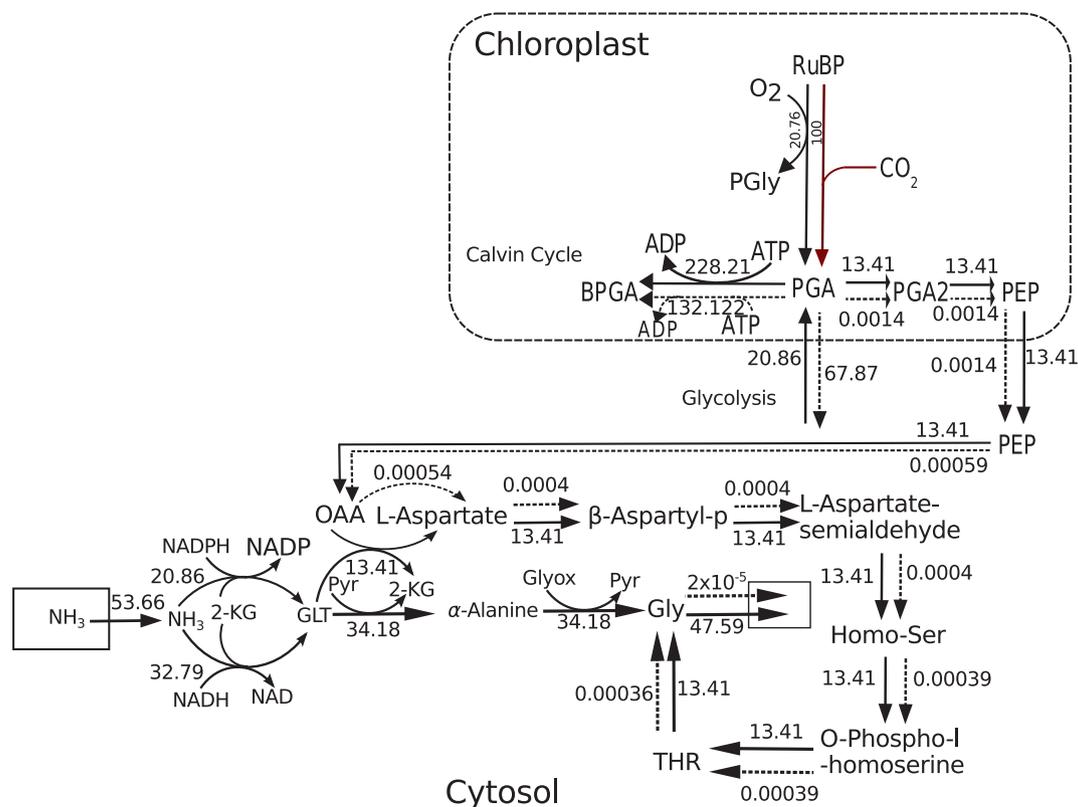
**Figure 4.** Flux distributions for high (solid) and low (dashed) glycine production. Small rectangular box at bottom left represents external nitrogen source.

(glutamate) in combination with OAA produces aspartate. The enzyme aspartate kinase plays an important role in homoserine biosynthesis by catalysing aspartate to β-Aspartyl-p (aspartyl-phosphate). Aspartate-semialdehyde dehydrogenase catalyses aspartyl-phosphate to L-aspartate-semialdehyde and homoserine dehydrogenase produces Homo-ser (homoserine). [The information about this pathway and associated genes in rice is also present in gramene (*http://pathway.gramene.org/RICE/NEW-IMAGE?type=PATHWAY&object=HOMOSERSYN-PWY*)]. Homo-ser is utilized in threonine biosynthesis pathway through an intermediate reaction which converts homo-ser to O-Phospho-l-homoserine that is catalysed by threonine synthase to produce THR (threonine) [*http://pathway.gramene.org/RICE/NEW-IMAGE?type=PATHWAY&object=HOMOSER-THRESYN-PWY*]. Finally, Gly is produced by threonine degradation pathway.

In case of maximum glycine production, there are mainly two sources of Gly production - (i) the pathway we already described and (ii) pathway involving cytosolic $NH_3$. This

$NH_3$ and 2-KG produce GLT. This GLT and cytosolic Pyr produce alanine which is converted to Gly.

3.2.4 *Glycine metabolism in cellular economy optimization:*
To understand the maximum Gly production under cellular economic condition, we used a method similar to the one described in section 3.2.2 (Algorithm 2), and the respective flux distribution is shown in figure 5. The main difference is that the $C_3$ carbon intermediate is transported through chloroplastidal GAP transporter instead of chloroplastidal PEP transporter. The participation of non-cyclic TCA cycle is also shown in figure 5.

### 3.3 *Carbon and nitrogen ratio*

Next, we calculated the variation of C/N (figure 6) which can be fixed by rice cellular metabolism to produce the biomass components. We observe the ratio (C/N) can vary from 1.71 to $13.35 \times 10^4$. First, we want to mention that our calculation was not able to estimate the actual range of C/N ratio. One of the main reasons is that we were simulating the metabolic
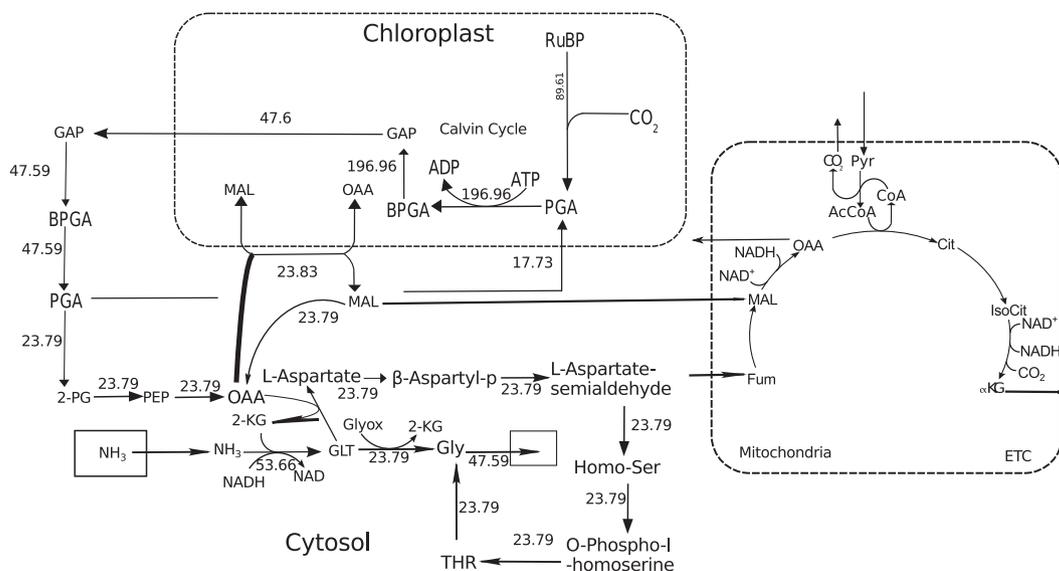
**Figure 5.** Glycine synthesis pathway when the flux of glycine is set to its maximum value and the objective is set to optimize cellular economy. ETC in the mitochondria was present and similar as shown in figure 3.

responses for some important biomass productions; several important secondary metabolites and other biomass components have not been included in our study. Moreover, we have not taken into account the effect of storage of different biomass components in sub-cellular compartments. However, it is interesting to note that under wide range of variations of ICT's transport activities; the ratio (C/N) was maximally populated at ~33 and this value was the same as



**Figure 6.** Carbon (C) to nitrogen (N) ratio in the entire range of simulations. Source of carbon is $CO_2$ and source of nitrogen is $NH_3$ and $NO_3$ intake. Axis X represents the ratio of carbon and nitrogen fluxes, whereas axis Y represents the number of occurrence of a particular value of C/N ratio in the entire simulations.

experimentally observed proportions which was used in our previous study (Poolman *et al.* 2013). At the same time, the results indicate that the intracellular transporters' transport capacities are coupled in such a way that a rice leaf cell maximally prefer to synthesize the biomass precursors in a fixed ratio of carbon and nitrogen.

### 3.4 *Maximization of sucrose production*

Rice plant transports the sucrose produced in a photosynthetic leaf to other tissues through phloem. As it is a major biomass compound involved in plant metabolism, it would be interesting to know whether the plant has the flexibility to produce higher amount of sucrose than experimentally observed proportion. We have observed that sucrose remains fixed in experimentally observed proportions in the entire range of simulations using biomass optimization criteria. Here, the effort is to find possible path and flux distribution which can produce higher sucrose in a given set of constraints. We set the lower bound of the flux of other biomass components, except sucrose, in the experimentally observed proportion and try to maximize only the sucrose production. The weight of each intracellular transporter is fixed to 1; i.e., each has equal capacity. Then the highest flux of sucrose is used in cellular economic condition. The obtained flux distribution is shown in figure 7. Sucrose is produced in cytosol. The main carbon source for its production is transported into the
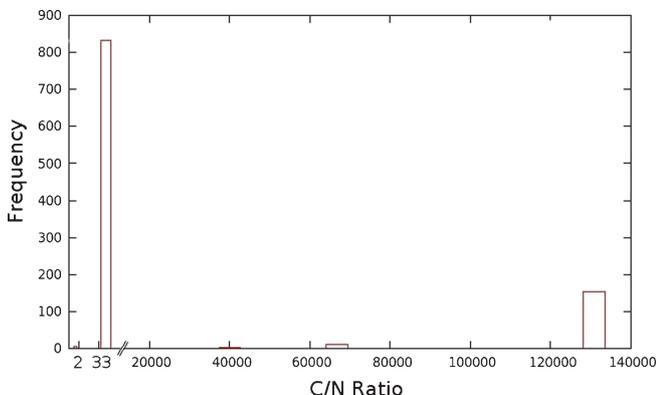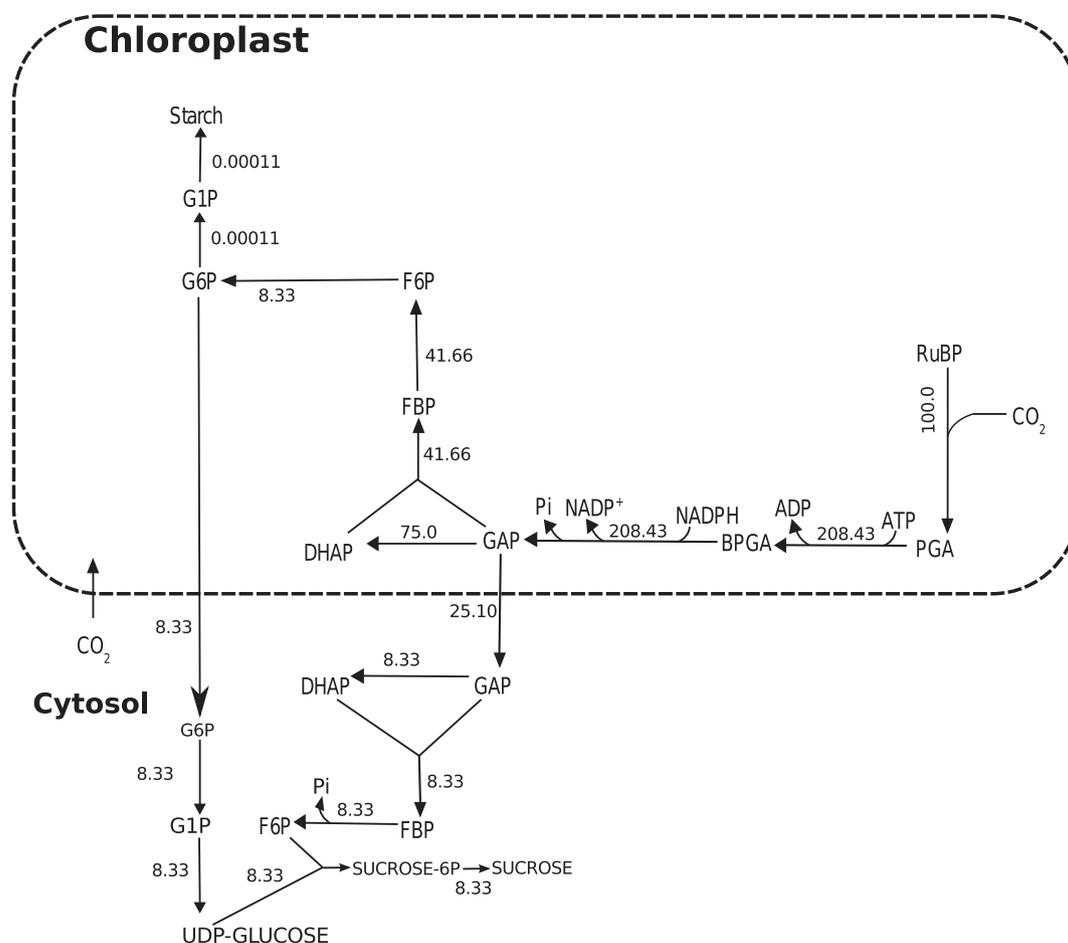
**Figure 7.** Path to produce maximum sucrose in an objective to optimize cellular economy.

cytosol through two chloroplastidal transporters -G6P and GAP transporters. Both these transporters transport carbon compounds to the cytosol and these are utilized to over-produce sucrose.

### 4. Discussion

We have used the flux balance analysis to predict the metabolic potential of rice cell to overproduce its biomass components. The results indicate that the rice metabolic network has the flexibility to overproduce its biomass components under biomass optimization criteria. On the other hand, we have also observed that while we simulate the metabolic responses for optimization of sucrose production, we get a maximum limit of sucrose when other biomass components are set to fixed values. We also demonstrated that change in optimization criteria gives one different possible solution.

This indicates that the plant, depending on its necessity and cellular condition (here, the enzymatic activity), can use different pathways. The wide variation in C/N ratio (with a lower and upper value) in the biomass suggests two points: (i) the rice plant has the flexibility to alter the amount of its biomass components in leaf and (ii) there is maximum and minimum range of C/N ratio by which the biomass production can be altered.

## References

Beyer P, Al-Babili S, Ye X, Lucca P, Schaub P, Welsch R and Potrykus I 2002 Golden rice: Introducing the β-carotene biosynthesis pathway into rice endosperm by genetic engineering to defeat vitamin a deficiency. *J. Nutr.* **132** 506S–510S

Cheung C, Williams TC, Poolman MG, Fell D, Ratcliffe RG, Sweetlove LJ, *et al*. 2013 A method for accounting for maintenance costs in flux balance analysis improves the prediction of plant cell metabolic phenotypes under stress conditions. *Plant J.* **75** 1050–1061

Edwards JS, Covert M and Palsson BO 2002 Metabolic modelling of microbes: the flux-balance approach. *Environ. Microbiol.* **4** 133–140

Fresco L 2005 Rice is life. *J. Food Compos. Anal.* **18** 249–253

Gnanamanickam SS 2009 Rice and its importance to human life; in *Biological control of rice diseases* pp 1–11

Herrgard MJ, Swainston N, Dobson P, Dunn WB, Arga KY, Arvas M, Bluthgen N, Borger S, *et al*. 2008 A consensus yeast metabolic network reconstruction obtained from a community approach to systems biology. *Nat. Biotechnol.* **26** 1155–1160

Jinhua X, Grandillo S, Ahn SN, McCouch SR, Tanksley SD, JiMing L, LongPing Y, *et al*. 1996 Genes from wild rice improve yield. *Nature* **384** 223–224

Kauffman KJ, Prakash P and Edwards JS 2003 Advances in flux balance analysis. *Curr. Opin. Biotechnol.* **14** 491–496

Orth JD, Thiele I and Palsson BO 2010 What is flux balance analysis? *Nat. Biotechnol.* **28** 245–248

Parry ML, Rosenzweig C, Iglesias A, Livermore M and Fischer G 2004 Effects of climate change on global food production under SRES emissions and socio-economic scenarios. *Glob. Environ. Chang.* **14** 53–67

Peng S, Khush GS, Virk P, Tang Q and Zou Y 2008 Progress in ideotype breeding to increase rice yield potential. *Field Crop Res.* **108** 32–38

Peralta-Yahya PP, Zhang F, Del Cardayre SB and Keasling JD 2012 Microbial engineering for the production of advanced biofuels. *Nature* **488** 320–328

Poolman MG 2006 ScrumPy: metabolic modelling with Python. *Syst. Biol.* **153** 375–378

Poolman MG, Bonde B, Gevorgyan A, Patel H and Fell D 2006 Challenges to be faced in the reconstruction of metabolic networks from public databases. *Syst. Biol.* **153** 379–384

Poolman MG, Kundu S, Shaw R and Fell DA 2013 Responses to light intensity in a genome-scale model of rice metabolism. *Plant Physiol.* **162** 1060–1072

Poolman MG, Miguet L, Sweetlove LJ and Fell DA 2009 A genome-scale metabolic model of Arabidopsis and some of its properties. *Plant Physiol.* **151** 1570–1581

Schuster S and Fell D 2007 Modeling and simulating metabolic networks; in *Bioinformatics-from genomes to therapies* pp 755–805

Shaw R and Kundu S 2013 Random weighting through linear programming into intracellular transporters of rice metabolic network; in *Pattern recognition and machine intelligence* 8251 pp 662–667

Simons M, Saha R, Amiour N, Kumar A, Guillard L, Clement G, Miquel M, Li Z, *et al*. 2014 Assessing the metabolic impact of nitrogen availability using a compartmentalized maize leaf genome-scale model. *Plant Physiol.* **166** 1659–1674

Sweetlove LJ, Beard KF, Nunes-Nesi A, Fernie AR and Ratcliffe RG 2010 Not just a circle: flux modes in the plant TCA cycle. *Trends Plant Sci.* **15** 462–470

Varma A and Palsson BO 1994 Stoichiometric flux balance models quantitatively predict growth and metabolic by-product secretion in wild-type Escherichia coli w3110. *Appl. Environ. Microbiol.* **60** 3724–3731

Vo TD, Greenberg HJ and Palsson BO 2004 Reconstruction and functional characterization of the human mitochondrial metabolic network based on proteomic and biochemical data. *J. Biol. Chem.* **279** 39532–39540